

# Nonlinear Effects of Zero-Crossing Detection Based Firing Angle Power Control on Lighting Performance

Dursun Kerem Karaduman <sup>1</sup>, Kenan Gençol <sup>2</sup> and Serkan Dişlitaş <sup>3</sup>

<sup>1</sup>Hitit University, Graduate School, Department of Interdisciplinary Energy Systems Engineering,19030, Corum, Türkiye, <sup>2</sup>Hitit University, Faculty of Engineering and Natural Sciences, Department of Electrical and Electronics Engineering,19030, Corum, Türkiye, <sup>3</sup>Hitit University, Faculty of Engineering and Natural Sciences, Department of Computer Engineering,19030, Corum, Türkiye.

**ABSTRACT** This paper presents the design, development, and performance evaluation of a single-phase microcontroller-based SCR (Silicon Controlled Rectifier) power control system employing a Zero-Crossing Detection (ZCD) technique for precise AC power regulation. The proposed embedded hardware architecture integrates a ZCD-based control unit, a bidirectional SCR driver circuit, and an SCR module with a power conditioning unit. The control algorithm, implemented on a microcontroller platform, performs precise zero-cross detection via hardware interrupts, computes the firing angle ( $\alpha$ ), and generates synchronized triggering pulses through optically isolated driver circuits. The system supports multiple operational modes, firing angle control, integral cycle control, and on/off control, enabling flexible load management. Experimental validation was performed using resistive loads and a 220 V, 42 W incandescent bulb. The results demonstrate accurate bidirectional triggering and stable load voltage control across firing angles from  $0^\circ$  to  $180^\circ$ , corresponding to delay times ( $t_d$ ) of 0–10 ms. Notably, the measured RMS voltage, apparent power and perceived illumination reached their peak at  $\alpha = 45^\circ$ , confirming a nonlinear relationship between the firing angle and output characteristics. The developed prototype provides rapid and stable power regulation between 0% and 100%, making it suitable for industrial heating and lighting systems. Future research will incorporate adaptive and soft-start control strategies to enhance operational efficiency and compatibility with resistive–inductive loads.

**KEYWORDS**  
Zero crossing detection  
Firing angle control  
Nonlinearity  
Embedded system

## INTRODUCTION

With the use of electrical energy, rapid and widespread technological advancements have emerged that facilitate our lives in every field, primarily in industry, healthcare, and education (Rashid 2014). The rapid increase in the global demand for electrical energy necessitates extensive research into the generation, transmission, distribution, utilization, and management of electrical energy in terms of efficiency, cost, and reliability (International Energy Agency 2023). The accurate control of the electrical power required in industrial and consumer electronics applications is a crucial subject that must first be investigated and developed (Bose 2020).

In this context, in industrial applications involving lighting, heating, and asynchronous motors, areas that constitute the main fields of electrical energy consumption, power control systems play a significant role in ensuring the smooth delivery of the required power to the load, the efficient and reliable use of energy, and overall energy savings. For this purpose, extensive theoretical and practical studies have been conducted on power control systems. Fundamentally, power electronic circuits form the basis of power control systems. A power electronic circuit essentially consists

of two main parts: the power section and the control section. In sectoral applications, various methods are employed to regulate the power supplied to the system through control circuits, which adjust it according to the requirements of the load (Bose 2020; Hart 2011; Rashid 2014).

Efficiency is a key issue in power control; however, preventing the occurrence of harmonic disturbances is also a critical problem that must be addressed. The use of mechanical relays in switching operations can cause arcing at peak voltage and lead to various related issues. Due to their advantages, such as the absence of moving parts, fast switching capability, and noiseless operation, semiconductor chips are preferred for power control and switching. In this regard, thyristor-based AC power control systems are widely used in industrial applications (Mauriac *et al.* 2004; Texas Instruments 2022).

In the literature, there are numerous studies focusing on the design, manufacturing, and performance enhancement of solid-state power control devices that employ methods such as Zero Crossing Detection (ZCD), phase control, and integral cycle control (Ashraf *et al.* 2020). Additionally, several studies have been conducted on ZCD-based approaches related to power control, management, and safety. For example, Al-Baihani *et al.* (2021) conducted a simulation and experimental modeling study on inverter triggering circuits using a microcontroller-based ZCD method. Kurak and Erdemir (2013) designed and simulated a triggering circuit based on the phase control principle of a PIC microcontroller-driven

**Manuscript received:** 28 November 2025,

**Revised:** 11 January 2026,

**Accepted:** 12 January 2026.

<sup>1</sup>dursunkaraduman05@gmail.com

<sup>2</sup>kenangencol@hitit.edu.tr (Corresponding author).

<sup>3</sup>serkandislitas@hitit.edu.tr

thyristor (SCR – Silicon-Controlled Rectifier). In a recent study, [Yurtcu \(2021\)](#) developed a fast and cost-effective hybrid system consisting of an electronic switch and a residual current circuit breaker, both operating on the principle of zero-cross detection, suitable for high-power applications. [Rustemli and Agrali \(2023\)](#) implemented a microcontroller-based application for the precise and practical speed control of AC universal motors via a computer interface using the firing angle control method to regulate motor power.

In thyristor-based power control circuits, performing zero-cross detection, adjusting necessary timing parameters, and driving operations complicate the design of the required electronic circuits. Therefore, using microcontroller-based zero-cross detection methods to drive SCRs simplifies the overall system structure. For this goal, in this study, a hardware and software-based embedded system design of a single-phase SCR-based power control device employing the ZCD method has been developed to achieve fast and efficient power control for industrial applications. The electrical performance characteristics of the developed prototype were obtained and analyzed.

The rest of the paper is organized as follows. The second section focuses on the basic principles and control methods of ZCD-based power control. The third section presents the hardware and software aspects of the designed and implemented microcontroller-based single-phase power control device operating on the ZCD method using SCRs. The fourth section analyzes the experimental performance of the developed system and presents the results. Finally, the paper is concluded by providing a general evaluation of the designed system and offering insights into its applicability and potential for further improvement.

## POWER CONTROL WITH ZERO CROSSING DETECTION (ZCD)

In this section, we describe the basic principles of ZCD and the power control methods employing ZCD. In particular, we focus on the firing angle control method which also forms the theoretical basis of the designed system in this study.

### Zero Crossing Detection

Zero Crossing Detection (ZCD) is the process of determining the precise instant at which the voltage of an AC sinusoidal signal crosses zero, either from the positive to the negative alternation or vice versa from the negative to the positive alternation. It is a method widely used in electronic power applications to synchronize control signals with the AC mains. In a sinusoidal waveform, zero crossing normally occurs twice during each cycle, once while the waveform rises and once while it falls ([Hart 2011; Zheng and Zhang 2012](#)).

Figure 1 illustrates the firing-angle-based triggering operation using the ZCD method. With the ZCD technique, both the falling (positive-to-negative) and rising (negative-to-positive) zero-crossing points of the supply signal within a period  $T$  are detected. According to the determined firing angle ( $\alpha$ ), a triggering signal is generated at the end of a corresponding firing delay ( $t_d$ ), allowing the SCRs to conduct in both the positive and negative triggering regions ([Hart 2011](#)).

Various solutions exist for performing ZCD and output triggering, including transistor-based, optocoupler-based, operational amplifier (OP-AMP)-based and microcontroller-based designs. Among them, microcontroller-based systems enable faster, more efficient, and more user-friendly control of the output power applied to the load through software-driven ZCD operation, ensuring

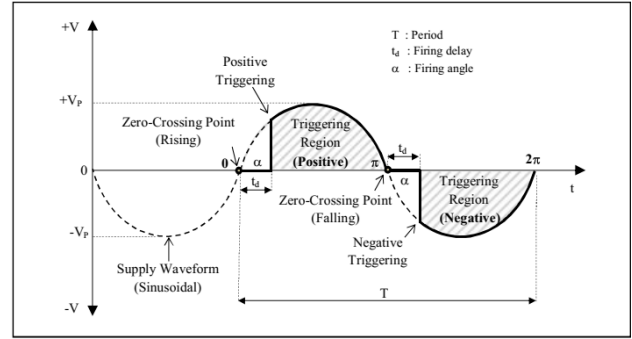


**Figure 1** Firing-angle triggering based on the ZCD method

that the desired power level is delivered more precisely ([Akyasan and Hasirci 2016; Bose 2020](#)).

In power control applications, various methods such as firing angle control, integral cycle control, and on/off control are employed based on the principle of thyristor triggering using the Zero Crossing Detection (ZCD) technique.

### Firing Angle Control Method

The fundamental principle of the firing angle control is that the triggering signal is applied after a predetermined delay time, corresponding to a specific firing angle ( $\alpha$ ) measured from the zero-crossing point of the AC supply that is determined by the ZCD method. This allows the output voltage to be applied to the load in proportion to the desired average power to be delivered. According to the method, the load voltage ( $V_L$ ) at the output, as a function of the supply peak voltage ( $V_p$ ) and the firing angle ( $\alpha$ ), can be expressed as in Eq. (1) ([Al-Mawsawi et al. 2012](#)):

$$V_{rms} = V_m \sqrt{\frac{1}{2\pi} \left( \pi - \alpha + \frac{1}{2} \sin(2\alpha) \right)} \quad (1)$$

This method enables precise regulation of the power delivered to the load, providing energy savings since only the required amount of current is utilized. It is primarily employed in inductive load applications, such as motors and transformers, but it can also be used with certain resistive loads where soft-start operation is desired to limit sudden inrush currents. However, due to the nature of phase control, the power factor is typically less than unity ( $\cos < 1$ ), and the method tends to generate a relatively high level of harmonic noise in the system ([Hart 2011; Rashid 2014; Texas Instruments 2022](#)).

Phase-angle control is widely used in heating, lighting, and similar AC load control applications because of its flexibility and responsiveness in adjusting power delivery. In general, this method is particularly advantageous in energy-saving applications, in systems that operate continuously for long durations, and in processes requiring stable operation. It is also suitable for environments where frequent ON/OFF switching of the system places stress on the power lines, where the supply voltage is unstable, or where a long operational lifetime of heating elements is desired ([Rashid 2014](#)). Figure 2 illustrates the output waveforms for different firing angles.

## THE DESIGNED SYSTEM

In this section, we present the hardware and software aspects of the designed and implemented microcontroller-based single-phase power control device operating upon the ZCD method using SCRs.

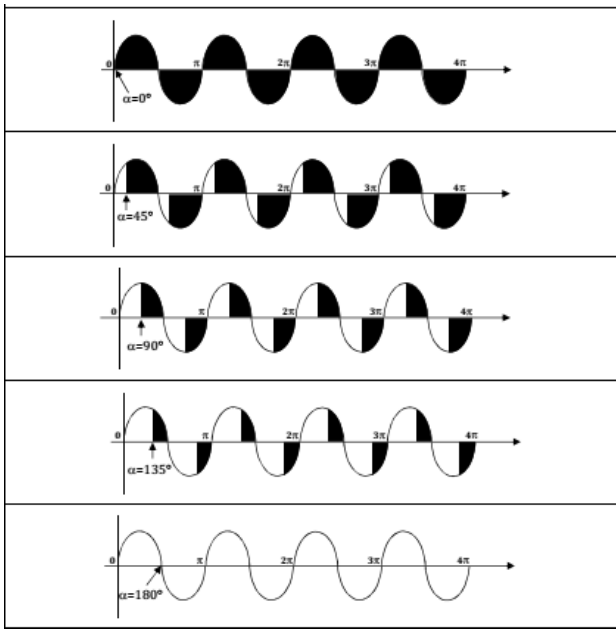


**Figure 2** Output waveforms of the supply signal under firing angle control

**System Hardware**

The general block diagram of the designed system is shown in Figure 3. The system consists of a ZCD-based control unit, an SCR driver unit, an SCR module, and a power unit.

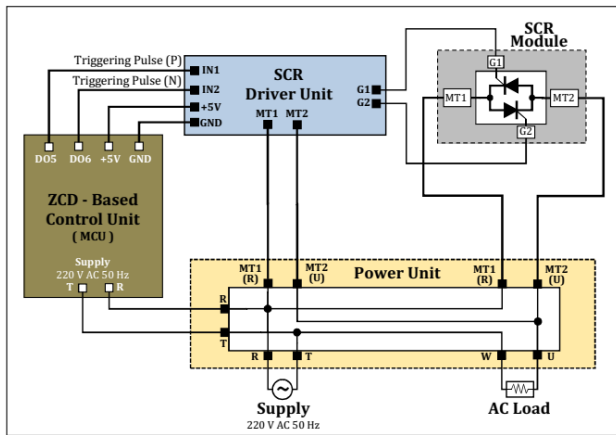


**Figure 3** General block diagram of the designed system

The ZCD-based control unit includes circuits responsible for generating rectified and ZCD signals from the mains voltage, as well as for receiving reference input values from the user, displaying them on the screen, and performing system control via a microcontroller-based platform as shown in Figure 4.

For AC power control, a dual-SCR module (IXYS MCC26-12io8B) with a current rating of 27 A and a voltage rating of 1.2 kV was employed in the designed system, as shown in Figure 5. In this SCR module, the G1 and G2 gate terminals (pins 5 and 6) are used for triggering the positive (+) and negative (-) alternations of the AC supply signal, respectively. Terminals 2 and 3 are connected together and used as MT1, while terminal 1 serves as MT2. With this configuration, the SCR module operates as two

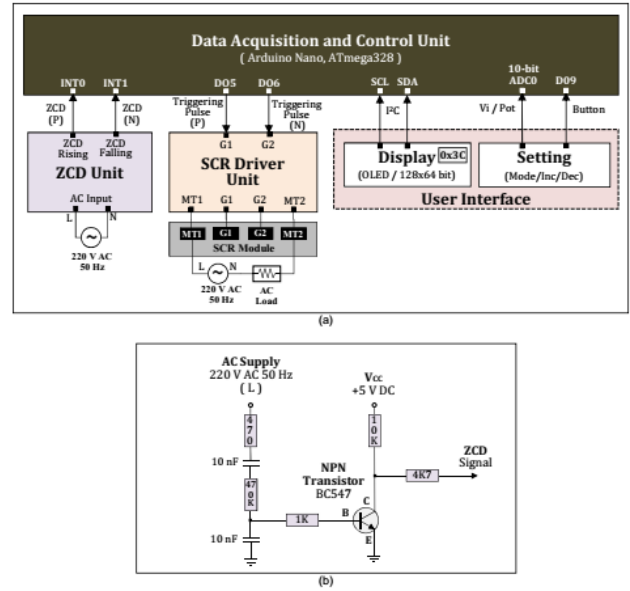


**Figure 4** ZCD based control unit (a) Block diagram (b) ZCD circuit

thyristors connected in anti-parallel, allowing bidirectional control of AC power.

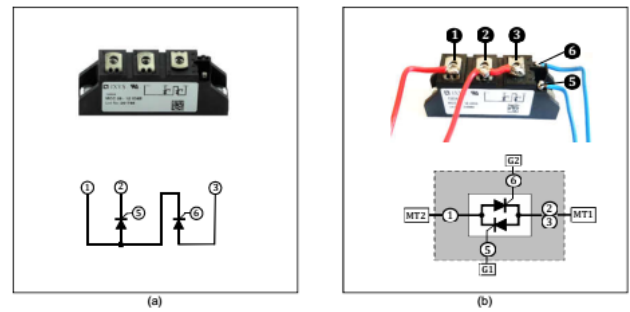


**Figure 5** Connection principles of the SCR module: (a) Standard module (b) Back-to-back connected module

To achieve power control on the load side, a microcontroller-based bidirectional SCR driver circuit was designed based on the Zero Crossing Detection (ZCD) method as shown in Figure 6. For each alternation (positive and negative) of the supply signal, the corresponding ZCD signals are detected through the INT0 and INT1 interrupt inputs of the microcontroller, triggered respectively by rising and falling edges. Based on the desired firing angle ( $\alpha$ ), the microcontroller calculates a delay time ( $t_d$ ), after which triggering pulses generated from digital output pins D5 and D6 are amplified through NPN transistors and applied to the G1 and G2 gate terminals of the two anti-parallel SCRs to initiate conduction. For galvanic isolation between the control and power circuits, optocoupler ICs with triac-triggered outputs were used. Diodes at the optocoupler outputs ensure unidirectional current flow, thus enabling single-direction triggering for each SCR. In the driver circuit, the AC supply and load are connected in series between the MT1 and MT2 main terminals of the SCRs. For proper operation, the L-phase of the mains source must be connected to the MT1 terminal, while the N-neutral line is connected to the MT2 terminal through the AC load.

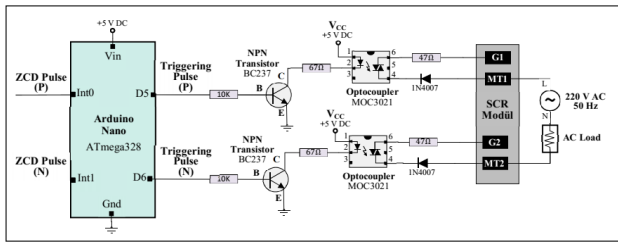


**Figure 6** Microcontroller based bidirectional SCR driver circuit employing the ZCD principle

### System Software

An embedded system software was developed for the SCR-based microcontroller power control system to perform data acquisition, system control, and the generation of triggering pulses according to the desired output power level or ratio determined from detected ZCD points. Figure 7 shows the flowchart of the embedded software algorithm designed to generate SCR triggering pulses using the ZCD method. At the start of execution, the algorithm receives reference configuration values such as power control mode, firing angle, and power ratio.

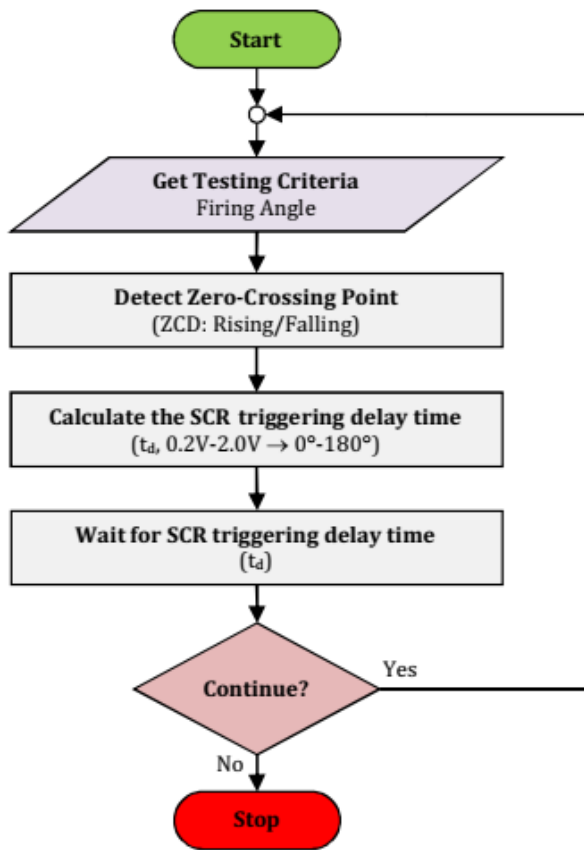


**Figure 7** General flowchart of the embedded system software

After initialization, the system identifies the zero-crossing points of the supply signal through rising and falling edge interrupts on the microcontroller's ZCD input pins. Depending on the selected power control mode, the system operates in firing angle control, integral cycle control, or on/off control.

In firing angle control mode, the microcontroller computes the

delay time ( $t_d$ ) corresponding to the desired firing angle between  $0^\circ$ – $180^\circ$ . After this delay, triggering pulses are generated at the output pins, turning on the SCRs. In integral cycle control mode, the microcontroller determines a cycle pattern according to the desired output power ratio (0–100%) and delivers triggering pulses for the selected cycles, ensuring conduction only during those intervals. In on/off control mode, the output is either enabled or disabled at the zero-crossing point depending on the state of the on/off control signal. The system operates continuously in this cyclic manner, updating its output according to user-defined control parameters.

### User Interface

In the designed system, an OLED LCD display was used for visualization purposes, a push-button was included to change the control mode, and a potentiometer was used to adjust the reference variable. Additionally, the required reference input voltage ( $V_i$ ) for adjustment can also be applied externally and directly to the analog input. To control the output according to the firing angle, the ADC0 analog input of the microcontroller with 10-bit resolution was utilized. Figure 8 (a) shows the variation in firing angle depending on the voltage  $V_i$  applied to the analog input. To prevent noise interference on the analog input, a lower threshold voltage of 0.2 V was implemented. For input voltages between 0.2 V and 2.0 V, the firing angle was adjusted within the range of  $0^\circ$  to  $180^\circ$ , with a sensitivity of 10 mV. Similarly, an upper threshold voltage of 2.0 V was defined to ensure that the firing angle could not exceed  $180^\circ$ .

Figure 8 (b) zooms in the OLED screen. The screen provides real-time information on the active power control mode (firing angle or integral cycle), the set firing angle, trigger delay time, desired output voltage ( $V_{out}$ ), and number of cycles applied to the load. According to the illustrated screen, the system is set to Firing angle Control mode, the firing angle is configured at  $90^\circ$ , the corresponding trigger delay time is 5000 s, thus, 50% of the supply signal is applied to the output. This user interface allows real-time monitoring and configuration of the system's power control parameters, providing both flexibility and operational transparency.

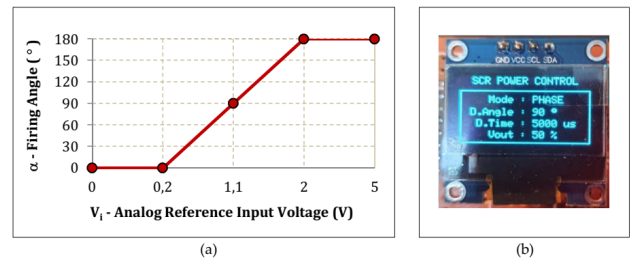


**Figure 8** (a) Firing angle variation relative to the  $V_i$  analog reference input voltage (b) Zoomed user screen

### EXPERIMENTAL RESULTS AND DISCUSSION

For the purpose of evaluating the performance of the designed system, the experimental setup shown in Figure 9 was constructed. In the setup, a Fluke 199C digital oscilloscope with a 200 MHz bandwidth and 2.5 GS/s sampling rate was used for signal measurements and waveform acquisitions. In addition, a True RMS digital multimeter was utilized to measure current and voltage values in order to determine the power delivered to the load. During the experimental studies, resistive loads of  $60 \Omega$ ,  $120 \Omega$ ,  $180 \Omega$ ,

and  $240\ \Omega$  (each rated at 700 W) were employed. Furthermore, a 220 V, 42 W incandescent bulb was used as an application-specific load to demonstrate the system's operational characteristics.

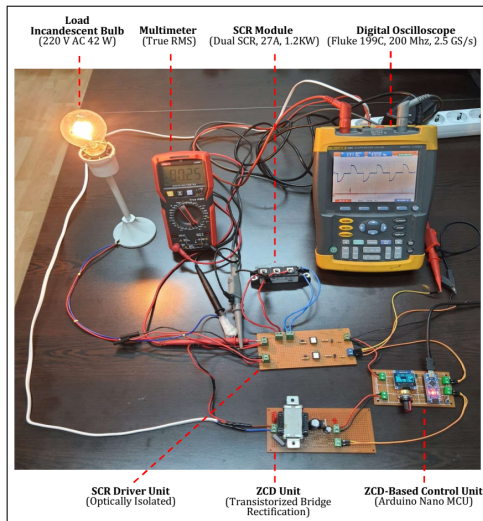


**Figure 9** Experimental setup

In the experimental study, the ZCD and SCR triggering signals were first examined. Figure 10 shows the ZCD signal and the corresponding SCR triggering signals obtained from the system in relation to the supply signal. In the microcontroller-based system, both the rising zero-crossing point and the falling zero-crossing point of the supply signal can be accurately detected using the ZCD signal. Depending on the system configuration, triggering pulses can be generated either simultaneously or independently for the rising and falling zero-crossing points. This allows the system to perform triggering selectively for only the positive alternation, only the negative alternation, or both positive and negative alternations of the AC supply signal, depending on the desired operation mode.

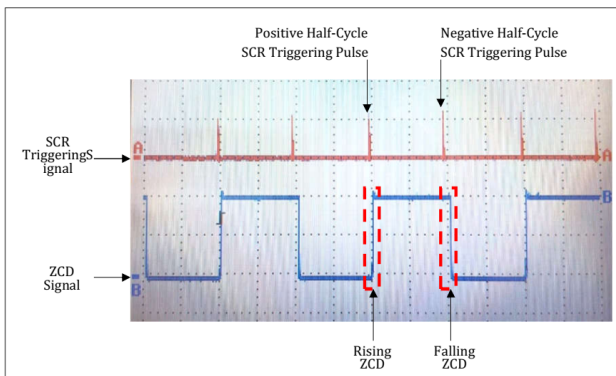


**Figure 10** ZCD and SCR triggering signals relative to the supply signal

Figure 11 illustrates the positive and negative triggering regions on the output signal obtained using the SCR triggering signals when the firing angle is set to  $90^\circ$ . Since the firing angle is  $90^\circ$ , the SCR triggering for both alternations is performed after a delay time ( $t_d$ ) of 5 ms for each half-cycle.

At the next stage of the experimental study, the triggering behavior of the SCR module was analyzed with respect to variations in the firing angle ( $\alpha$ ). For this purpose, resistive loads ranging from

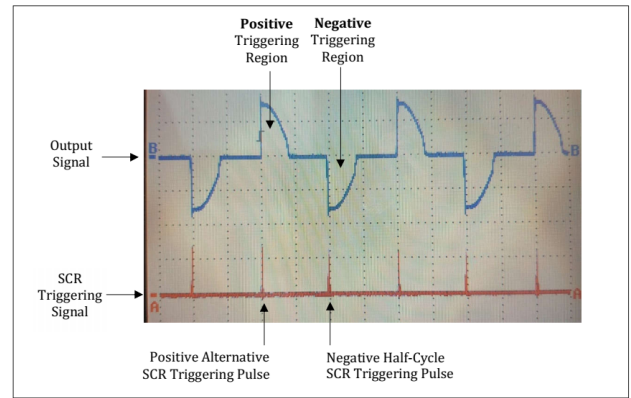


**Figure 11** Positive and negative triggering regions on the output signal at the firing angle  $90^\circ$

$60\ \Omega$  to  $240\ \Omega$ , each rated at 700 W, were connected to the SCR module. Depending on the firing angle variation between  $0^\circ$  and  $180^\circ$ , the SCR module was triggered after the corresponding delay times (td) for both alternations of the supply signal. Consequently, the AC voltage ( $V_{rms}$ ) and current ( $I_{rms}$ ) values across the load were measured and recorded, as presented in Table 1. Figure 12 shows that as the firing angle increases, the voltage applied to the load decreases. When  $\alpha = 0^\circ$ , the source current is directly transferred to the output, whereas at  $\alpha = 180^\circ$ , the output voltage drops to 0 V. Figure 13 presents the variation of the apparent power (S) calculated from the measured voltage and current values across the load. It is observed that as the firing angle increases, the apparent power on the load gradually decreases, reaching 0 VA when  $\alpha = 180^\circ$ .

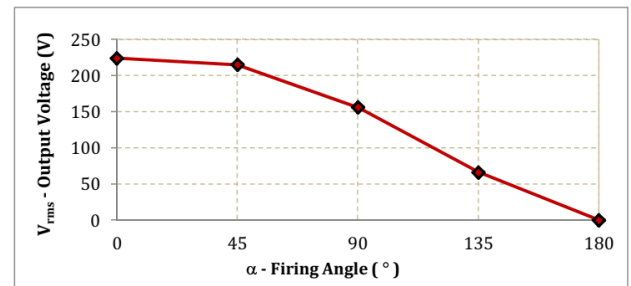


**Figure 12** Variation of  $V_{rms}$  output voltage with respect to firing angle

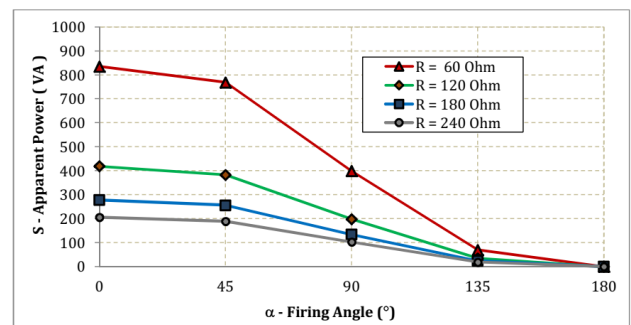


**Figure 13** Variation of apparent power delivered to different loads with respect to firing angle

**Table 1** Variation of electrical parameters for different resistive loads under SCR triggering

$\alpha$ ( $^\circ$ )	$t_d$ ( $\mu$ s)	$R_L = 60 \Omega$			$R_L = 120 \Omega$			$R_L = 180 \Omega$			$R_L = 240 \Omega$		
		$V_{rms}$ (V)	$I_{rms}$ (A)	$S$ (VA)	$V_{rms}$	$I_{rms}$	$S$	$V_{rms}$	$I_{rms}$	$S$	$V_{rms}$	$I_{rms}$	$S$
0	0	224	3.73	835.52	224	1.87	418.88	224	1.24	277.76	224	0.92	206.08
45	2500	215	3.58	769.70	215	1.78	382.70	215	1.19	255.85	215	0.88	189.20
90	5000	156	2.56	399.36	156	1.27	198.12	156	0.86	134.16	156	0.66	102.96
135	7500	66	1.06	69.96	66	0.53	34.98	66	0.36	23.76	66	0.29	19.14
180	10000	0	0	0	0	0	0	0	0	0	0	0	0

In the last stage of the experimental study, which focuses on the practical application of the system, the triggering of the SCR module and the performance of an incandescent bulb were analyzed in relation to changes in the firing angle ( $\alpha$ ). For this purpose, a 220 V, 42 W AC incandescent bulb was used as the load in the system. Accordingly, depending on the firing angle variation between  $0^\circ$  and  $180^\circ$ , the SCR module was triggered following the corresponding delay time ( $t_d$ ), and the resulting  $V_{rms}$  and  $I_{rms}$  values across the lamp were measured and given in Table 2. Figure 14 shows that as the firing angle increases, the voltage applied to the load decreases. When  $\alpha = 0^\circ$ , the source voltage is directly transferred to the output, whereas at  $\alpha = 180^\circ$ , the source voltage becomes 0 V. Figure 15 presents the variation of the apparent power ( $S$ ) calculated from the measured current and voltage values as a function of the firing angle. It is observed that the maximum apparent power on the load occurs at  $\alpha = 45^\circ$ , at which point the incandescent bulb produces its maximum illumination, which is also clearly visible during the experiment.

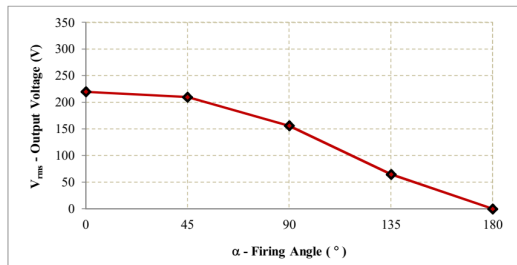


**Figure 14** Variation of output RMS voltage ( $V_{rms}$ ) applied to the incandescent bulb with respect to firing angle

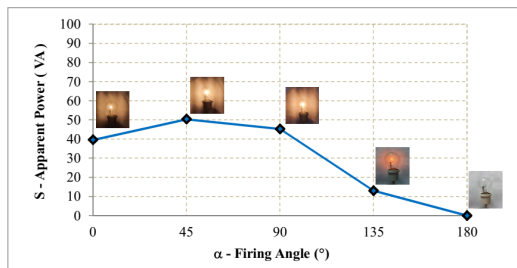


**Figure 15** Variation of apparent power delivered to the incandescent bulb with respect to firing angle

For different firing angle ( $\alpha$ ) values of  $0^\circ$ ,  $45^\circ$ ,  $90^\circ$ ,  $135^\circ$ , and  $180^\circ$ , the corresponding SCR triggering signals, output waveforms, control unit display screenshots, and the illumination levels of

the incandescent bulb used as the load are shown in Figure 16 (a) through (d), respectively. According to these firing angle values, the corresponding triggering delay times ( $t_d$ ) are 0 s, 2500 s, 5000 s, 7500 s, and 10000 s, respectively.

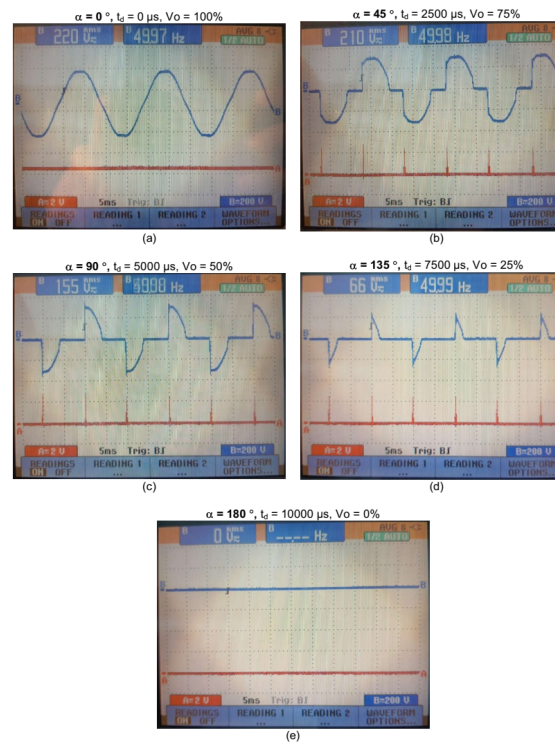


**Figure 16** SCR triggering and output signals as a function of various firing angle values between  $0^\circ$  and  $180^\circ$

**Table 2** Electrical parameters of the incandescent bulb (220 V, 42 W) under SCR firing angle control

$\alpha$ ( $^\circ$ )	$t_d$ ( $\mu$ s)	$V_{rms}$ (V)	$I_{rms}$ (A)	$S$ (VA)
0	0	220	0.18	39.60
45	2500	210	0.24	50.40
90	5000	156	0.29	45.24
135	7500	65	0.20	13.00
180	10000	0	0	0

## CONCLUSION

In this study, the hardware and software of an embedded system of a single-phase microcontroller-based SCR power control device was developed to achieve fast and efficient power control for industrial applications. Using the ZCD method, the system enables bidirectional triggering of two anti-parallel connected SCRs after a delay time corresponding to the desired firing angle, thereby controlling the power applied to the load. In the designed system, firing angle control of the load is performed through the microcontroller's analog input via the SCR module. To prevent noise interference on the analog input, lower and upper threshold voltages were defined for the 10-bit resolution analog input of the microcontroller. By applying an input voltage between 0.2 V and 2.0 V, the corresponding firing angle ( $\alpha$ ) is adjusted within the range of  $0^\circ$  to  $180^\circ$ , with a precision of 10 mV.

To evaluate the performance of the designed system, an experimental setup was established in which the current and voltage measurements of the control and power circuits, as well as the corresponding signal waveforms, could be analyzed. In the experimental study, for a mains frequency of 50 Hz, the SCR triggering delay time ( $t_d$ ) was adjusted between 0 and 10 ms corresponding to firing angle ( $\alpha$ ) variations from  $0^\circ$  to  $180^\circ$ , thereby enabling control of the power applied to the load between 0% and 100%. Within the scope of the application, a 220 V, 42 W AC incandescent bulb was employed as the load. By driving the lamp according to the firing angle control based on the ZCD method, different power levels were delivered to the load.

It was observed that although the firing angle varied linearly between  $0^\circ$  and  $180^\circ$ , the applied power did not change linearly, resulting in a nonlinear relationship between the firing angle and the illumination level of the incandescent bulb. Notably, the maximum perceived illumination on the lamp was observed at a firing angle of  $45^\circ$ . Unlike theoretical models that predict a monotonic decrease in power and illumination, these experimental findings highlight the importance of empirical validation. Whether this observed peak at intermediate angles originates from the inherent dynamic nature of the load, the impact of high-order harmonic distortion on measurement instrumentation, or potential measurement limitations remains a subject for further investigation. Future studies should aim to clarify these factors to enhance the precision of diagnostic accuracy in phase-controlled systems.

As a result, it has been demonstrated that the developed power control device can achieve fast and stable power regulation between 0% and 100% in industrial applications such as lighting and heating. In future, the functionality of the system can be further expanded by implementing additional software modules such as integral cycle control, on/off control, and soft-start operation, in addition to the existing firing angle control. These enhancements would significantly broaden the applicability of the device to a wide range of industrial environments involving resistive, inductive, and capacitive loads, thereby improving its adaptability, energy efficiency, and operational flexibility.

## Ethical standard

The authors have no relevant financial or non-financial interests to disclose.

## Availability of data and material

The data that support the findings of this study are available from the corresponding author upon reasonable request.

## Conflicts of interest

The authors declare that there is no conflict of interest regarding the publication of this paper.

## LITERATURE CITED

- Akyasan, M. and U. Hasirci, 2016 Farkli sifir gecis algilama devrelerinin deneysel performansinin incelenmesi. *Ileri Teknoloji Bilimleri Dergisi* 5.
- Al-Baihani, H. H., S. Eskander, M. A. Elsayess, E. Gouda, M. Ammar, *et al.*, 2021 Simulation and experimental modeling of inverter triggering circuits using zero-crossing detector (zcd) based on microcontroller. *Mansoura Engineering Journal* 46: 1–10.
- Al-Mawsawi, S. A., N. Allaith, H. Qassim, and S. Dhiya, 2012 An accurate formula for the firing angle of the phase angle control in terms of the duty cycle of the integral cycle control. *Journal of Automation and Systems Engineering*.
- Ashraf, N., T. Izhar, G. Abbas, A. B. Awan, A. S. Alghamdi, *et al.*, 2020 A new single-phase direct frequency controller having reduced switching count without zero-crossing detector for induction heating system. *Electronics* 9: 430.
- Bose, B. K., 2020 *Power Electronics and Motor Drives: Advances and Trends*. Academic Press, second edition.
- Hart, D. W., 2011 *Power Electronics*. McGraw-Hill Education.
- International Energy Agency, 2023 World energy outlook 2023.
- Kurak, E. and V. Erdemir, 2013 Design and implementation of scr trigger circuit using microcontrollers. *Electronic Journal of Vocational Colleges* 3: 104–109.
- Mauriac, C., Y. Raingeaud, J. Baillou, L. Gonthier, and R. Pezani, 2004 Thyristors and triacs control by a high frequency sine signal. In *IEEE International Symposium on Industrial Electronics*, volume 2, pp. 1029–1033, IEEE.
- Rashid, M. H., 2014 *Power Electronics: Devices, Circuits, and Applications*. Pearson, fourth edition.
- Rustemli, S. and E. Agrali, 2023 Computer based speed control application for universal motor. *MANAS Journal of Engineering* 11: 112–118.
- Texas Instruments, 2022 Zero-cross switching for solid-state relays reference design. Technical Report TIDA-050058, Texas Instruments.
- Yurtcu, A., 2021 *Sifir Gecis Tabanlı Elektronik Salter ve Kacak Akım Roleli Hibrit Bir Sistemin Gelistirilmesi*. Ph.D. thesis, Istanbul Gedik University.
- Zheng, G. L. and Z. F. Zhang, 2012 A novel intelligent load control switch based on dynamic compensation method for current zero-crossing point. *Advanced Materials Research* 433: 4717–4724.

**How to cite this article:** Karaduman, D. K., Gencol, K., and Dislitas, S. Nonlinear Effects of Zero-Crossing Detection Based Firing Angle Power Control on Lighting Performance. *Chaos and Fractals*, 3(1), 54-60, 2026.

**Licensing Policy:** The published articles in CHF are licensed under a [Creative Commons Attribution-NonCommercial 4.0 International License](https://creativecommons.org/licenses/by-nc/4.0/).

